#### (12) INTERNATIONAL APPLICATION PUBLISHED UNDER THE PATENT COOPERATION TREATY (PCT)

(19) World Intellectual Property Organization

International Bureau





(10) International Publication Number WO 2016/157083 A1

6 October 2016 (06.10.2016)

(43) International Publication Date

(51) International Patent Classification: H01M 10/0562 (2010.01)

H01M 4/133 (2010.01) H01M 4/136 (2010.01)

H01M 4/38 (2006.01)

H01M 4/587 (2010.01) **H01M 4/66** (2006.01) H01M 10/054 (2010.01) H01G 9/025 (2006.01) H01G 9/15 (2006.01) H01M 2/02 (2006.01)

H01G 9/00 (2006.01)

(21) International Application Number:

PCT/IB2016/051776

(22) International Filing Date:

29 March 2016 (29.03.2016)

(25) Filing Language:

English

(26) Publication Language:

English

(30) Priority Data:

108327 27 March 2015 (27.03.2015) PT

- (72)Inventor; and
- Applicant: SOUSA SOARES DE OLIVEIRA BRAGA, Maria Helena [PT/PT]; Rua De Salgueiros, 651, 4050-533 Porto (PT).
- (72) Inventors: DO AMARAL FERREIRA, José Jorge; Rua Dr. Afonso Cordeiro, 420, 4ºesq, 4450-003 Matosinhos (PT). MURCHISON JR, Andrew Jackson; 6225 Culvert Drive, San Jose Ca., California 95123 (US).

- Agent: TEIXEIRA DE CARVALHO, Anabela; Patentree, Edificio Net, Rua de Salazares 842, 4149-002 Porto
- (81) Designated States (unless otherwise indicated, for every kind of national protection available): AE, AG, AL, AM, AO, AT, AU, AZ, BA, BB, BG, BH, BN, BR, BW, BY, BZ, CA, CH, CL, CN, CO, CR, CU, CZ, DE, DK, DM, DO, DZ, EC, EE, EG, ES, FI, GB, GD, GE, GH, GM, GT, HN, HR, HU, ID, IL, IN, IR, IS, JP, KE, KG, KN, KP, KR, KZ, LA, LC, LK, LR, LS, LU, LY, MA, MD, ME, MG, MK, MN, MW, MX, MY, MZ, NA, NG, NI, NO, NZ, OM, PA, PE, PG, PH, PL, PT, QA, RO, RS, RU, RW, SA, SC, SD, SE, SG, SK, SL, SM, ST, SV, SY, TH, TJ, TM, TN, TR, TT, TZ, UA, UG, US, UZ, VC, VN, ZA, ZM, ZW.
- (84) Designated States (unless otherwise indicated, for every kind of regional protection available): ARIPO (BW, GH, GM, KE, LR, LS, MW, MZ, NA, RW, SD, SL, ST, SZ, TZ, UG, ZM, ZW), Eurasian (AM, AZ, BY, KG, KZ, RU, TJ, TM), European (AL, AT, BE, BG, CH, CY, CZ, DE, DK, EE, ES, FI, FR, GB, GR, HR, HU, IE, IS, IT, LT, LU, LV, MC, MK, MT, NL, NO, PL, PT, RO, RS, SE, SI, SK, SM, TR), OAPI (BF, BJ, CF, CG, CI, CM, GA, GN, GQ, GW, KM, ML, MR, NE, SN, TD, TG).

#### Published:

with international search report (Art. 21(3))



(54) Title: AN ELECTROCHEMICAL SOLID CARBON-SULFUR NA-ION BASED DEVICE AND USES THEREOF

(57) Abstract: The present disclosure relates to the development layered electrochemical solid devices, in particular to the development of a new device; a supercapacitor and or a battery solid carbon- sulfur Na-ion glassy electrolyte based device with autonomous dual functionality comprising a safe, environmentally friendly and inexpensive device. The present subject-matter relates to a layered electrochemical solid device comprising a positive electrode current collector, a positive electrode, a glass electrolyte, a negative electrode and a negative electrode current collector wherein the positive electrode current collector comprises aluminum; the positive electrode comprises sulfur, glass electrolyte and carbon; the electrolyte composition comprises a compound of formula Na<sub>3-2x</sub>M<sub>x</sub>-HalO or Na<sub>3</sub>- 3xMxHalO wherein: M is selected from the group consisting of boron, aluminum, magnesium, calcium, strontium, barium; Hal is selected from the group consisting of fluoride, chloride, bromide, iodide or mixtures thereof; X is the number of moles of M and  $0 \le x \le 0.01$ ; the negative electrode comprises a carbonaceous material; the negative electrode current collector comprises copper. The present subject-matter relates to a layered electrochemical solid device comprising the above described layers with inverted roles.

#### DESCRIPTION

### AN ELECTROCHEMICAL SOLID CARBON-SULFUR NA-ION BASED DEVICE AND USES THEREOF

#### **Technical field**

[0001] The present disclosure relates to the development and improvement of sodium-ion electrochemical devices, in particular to the development of a new device; a supercapacitor and a supercapacitor and battery solid carbon-sulfur Na-ion based device with autonomous dual functionality which is charged from the Na-rich glassy electrolyte solid electrolyte glass comprising a safe, environmentally friendly and inexpensive device. The present dual mode of operation, both a high energy battery mode and power capacity supercapacitor mode along with a burst discharge of less or equal to 1 second. In the supercapacitor mode of a device, it can store more energy than any other known capacitor and in the battery mode several of the present devices stored more energy for a longer period than most Na-ion batteries.

## **Background Art**

[0002] Since the advent of energy storage, humankind has been seeking a combined high power, high energy storage solution in a single device. Considerable efforts have been expended on the development of high-performance energy-storage devices such as Lithium-ion capacitors (LICs), Lithium-ion batteries (LIBs) and, lately, Sodium-ion batteries (NIBs). High performance energy storage devices such as supercapacitors and batteries rely on different fundamental working principles - bulk versus surface - electron conduction and/or ion diffusion corresponding to electrochemical versus electrostatic energy storage (1). Electric double-layer capacitors (EDLCs), which store energy through accumulation of ions on the electrodes' interface, have low energy storage capacity but very high power density. However, in hybrid capacitors (1-5) like LICs, despite their recent advancement, the imbalance in kinetics between the two electrodes still remains a major drawback. Here it is presented an energy storage cell with two energy storage modes which can operate as a supercapacitor or a supercapacitor and sodium battery (6-8);

[0003] This device will impact a very broad spectrum of applications especially in the transportation, grid stationary, and aerospace.

[0004] Ford Motor pioneered the molten salt Na-S battery in Ford's "Ecostar" 1971, to power early-model electric cars (9). Lately, developments with NASICON membrane allowed operation at 90 °C with all components remaining solid (10). Because of its high energy density, the Na-S battery has been proposed for space applications (11,12). Sodium-sulfur cells can be made space-qualified; in fact a test Na-S r cell was flown on the Space Shuttle. The Na-S flight experiment demonstrated a battery with a specific energy of 150 Wh/kg (3 x Ni–MH battery energy density), operating at 350 °C. It was launched on the STS-87 mission in November 1997, and demonstrated 10 days of experiment operation in orbit (13). As highlighted above, molten salt Na-S batteries can be deployed to support the electric grid. In 2010, Presidio, Texas built the world's largest sodiumsulfur battery, which can provide 4 MW of power for up to eight hours when the city's lone line to the Texas power grid goes down (14). Under some market conditions, Na-S batteries provide value via energy arbitrage (charging battery when electricity is abundant/cheap, and discharging into the grid when electricity is more valuable) and voltage regulation (15). Na-S batteries are a possible energy storage technology to support renewable energy generation, specifically wind farms and solar generation plants. In the case of a wind farm, the battery would store energy during times of high wind but low power demand. This stored energy could then be discharged from the batteries during peak load periods. In addition to this power shifting, it is likely that Na-S batteries could be used throughout the day to assist in stabilizing the power output of the wind farm during wind fluctuations. These types of batteries present an option for energy storage in locations where other storage options are not feasible. For example, pumped-storage hydroelectricity facilities require significant space and water resources, while compressed air energy storage (CAES) requires some type of geologic feature such as a salt cave (16).

[0005] Sodium-ion batteries (NIBs) have been gaining increasing attention thanks to the natural abundance and low toxicity of sodium resources (6-8). Furthermore, sodium is located just below lithium in the *s* block. Therefore, similar chemical approaches including a synthetic strategy, intercalation/alloying/conversion chemistry, and characterization methods utilized in electrode materials for LIBs could be applied to develop electrode materials for NIBs. Despite potential disadvantages, including larger size (0.98-1.02 Å) of Na cations (approximately, 20-25% larger than Li cations, 0.76-0.78 Å) and higher redox potential (-2.71 V vs. SHE) of Na/Na<sup>+</sup> compared to Li analogues (-3.04 V vs. SHE) of Li/Li<sup>+</sup> (17), the different interactions between the guest Na-cations and the host crystal structures can influence the kinetics as well as thermodynamic properties of NIBs, and this may provide an avenue for a breakthrough technology to surpass LIBs (18). As an effort to find alternatives to graphite in NIBs, Doeff et al. demonstrated the reversible de/insertion

of Na ions into disordered carbons for an anode in NIBs (19). Most of the sodium ions are electrochemically inserted into nanoporous voids of hard carbon (HC), which is built by disordered graphene stacking – the so-called 'house of cards' type model. Two independent research groups lead by Dahn (20) and Tirado (21) demonstrated that the initial specific capacity of hard carbon in NIBs is ca. 300 mAh/g close to that of graphite in LIBs. Most of the reversible capacity is related to sodium storage inside nanocavities. However, this hard carbon electrode exhibited significant loss of capacity within 10 cycles with poor rate performance.

[0006] In the simplest configuration an EDLC consists of two electrodes immersed into a liquid electrolyte and separated by a membrane. Upon application of a voltage difference to the electrodes, the ions of the opposite charge of the electrolyte accumulate on the electrodes' interface in a quantity proportional to the applied voltage, forming a double layer capacitor (2). The charge storage mechanism in a typical EDLC is not Faradaic, which means that during the charge and discharge of this type of device, no charge transfer takes place across the electrolyte/electrode interface and the energy storage is of an electrostatic nature. In LICs, electrodes' carbonaceous materials may additionally exhibit chemical interactions with selected electrolytes, which involve fast and often reversible charge-transfer reactions between the carbon surface and the electrolyte ions; such processes are Faradaic. At a constant temperature and voltage, the ionic density on the carbon electrode surface is controlled by a balance between the changes in entropy and enthalpy of the system (3). The sodium ion capacitors, NICs, were not studied in detail; it is expected that some of their properties can be inferred from LICs properties. The maximum voltage in an EDLC is generally determined by the electrochemical stability window of the selected electrolyte. Impurities and functional groups on carbon, however, may catalyze electrolyte decomposition, narrowing the operating voltage window.

[0007] Batteries on the other hand are composed by electrochemical cells. Each cell consists of positive and negative electrode separated by an electrolyte. Once the electrodes are connected externally, there are chemical reactions that occur at both electrodes, liberating electrons and enabling the current to be tapped by the user (22).

[0008] These facts are disclosed in order to illustrate the technical problem addressed by the present disclosure.

#### **General Description**

[0009] The present disclosure relates to the development and improvement of sodium-ion electrochemical devices, in particular to the development of a new device, a supercapacitor and battery solid carbon-sulfur Na-ion based device with autonomous dual functionality which is uniquely charged from the Na-rich glassy electrolyte solid electrolyte glass comprising a safe, environmentally friendly and inexpensive device. In the supercapacitor mode of a device, it can store more energy than any other known capacitor and in the battery mode several of devices stored more energy for a longer period than most Na-ion batteries.

[0010] In an embodiment, the present disclosure relates to a supercapacitor and battery solid carbon-sulfur Na-ion based device with autonomous dual functionality and charged from the Narich glassy electrolyte.

[0011] In some cases, the collectors can have a predominant role. They can function as electrodes being the copper + carbon black the positive electrode and the sulfur + glass electrolyte + carbon in aluminum the negative electrode. This configuration makes the device works reversely to what was described for charge and discharge.

[0012] A supercapacitor and battery solid carbon-sulfur Na-ion based device with autonomous dual functionality which is uniquely charged from the Na-rich glassy electrolyte is now disclosed. Unlike the molten salt battery, Na-S, constructed from liquid sodium and sulfur, which operates at temperatures of 300 to 350 °C and generates highly corrosive sodium polysulfides, and therefore primarily suited to large-scale non-mobile applications such as grid energy storage; the devices now disclosed are environmentally friendly and inexpensive and so not present any of the previous cited risks of molten Na-S batteries. They operate at room temperature and do not exhibit any polysulfides 'shuttle' problems associated with this chemistry, and therefore these devices have a prolonged cycle life. They present a dual mode of operation, both a high energy battery mode and a power capacity supercapacitor mode along with a burst discharge of one (1) second.

[0013] In the supercapacitor mode of a device, it can store more energy than any other known capacitor and in the battery mode, the devices now disclosed stored more energy for a longer period than most Na-ion batteries. The devices now disclosed are safe and therefore will have numerous advantages in a multitude of markets such as mobile applications and grid energy storage.

[0014] A supercapacitor and battery solid carbon-sulfur Na-ion based device with autonomous dual functionality and charged from the Na-rich glassy electrolyte are now disclosed.

[0015] This disclosure presents a solid state bulk energy storage device working autonomously, simultaneously or independently as a supercapacitor and as a battery; although predominantly as a supercapacitor. On charge, the supercapacitor is the last mode to be fully charged and on discharge, the supercapacitor mode is the first to be discharged. The device is composed of a copper bulk collector, a negative electrode of carbon black (C) which is mostly disordered graphite (Fig. 1), a doped glassy electrolyte Na<sub>3</sub>ClO based, a positive electrode comprised of a mixture of: sulfur (S<sub>8</sub>), a glassy electrolyte, and carbon black, deposited on an aluminum bulk collector. If some sulfur reacts with the electrolyte, during electrode preparation, it is most likely just at the surface forming an amorphous phase that cannot be distinguished from the other amorphous phases already present (glassy electrolyte and carbon black, Fig. 1). The surface dimensions of the cells' electrodes are 2.5×2.5 cm<sup>2</sup> with a loading of 0.20-0.40 g/cm<sup>2</sup> of electrode materials and electrolyte. The sulfur loading can be 0.018-0.040 g/cm<sup>2</sup>. Collectors have an extended functionality; besides being an electronic transport media, they have a support and heat dissipation functionality which is not intrinsic to the device. The cells have 0.15-0.35 g/cm<sup>2</sup> of electrolyte as separator. The cell's thickness is 0.15-0.35 cm. The electrodes, electrolyte and collectors were accountable to the device's weight.

[0016] A glassy-electrolyte of the same family, Li<sub>3</sub>ClO, was previously characterized (23).

[0017] The Na<sub>3</sub>CIO based glassy electrolyte's high ionic conductivity enables the fabrication of solid state energy devices with bulk (thick) layers of electrolyte, enabling existing battery coating methods. The Na-rich transport characteristics of the electrolyte permit enhanced cell component kinetics and increased life cycle. Moreover, the battery mode is charged/discharged from the electrolyte and in the sulfur<sub>based</sub> electrode the Na-ions do not cross the electrode's surface allowing for a new set of electrode combinations such as the carbon-sulfur pair presented herein. The open circuit's voltage at the time of cell fabrication, is lower than 0.1 V permitting for extremely safe transportation and storage. Consequently, the device can be charged at the destination as battery or/and supercapacitor.

[0018] The galvanostatic charge/discharge cycles for the carbon(C)/electrolyte/sulfur<sub>based</sub>(S) - device 1@a are shown in Fig. 2, at a charging current of 25 mA, 15 mA/g<sub>cell</sub> and discharging at an open circuit. The EDLCs within device 1@a begin to charge at  $\Delta V = 1.4$  V and the EDLC mode is the only mode charged in all the curves in Fig. 2 and 3. This latter observation is reinforced by analyzing the device's discharge data; the device discharges to 0 V, not presenting any battery mode discharge. It is highlighted the high capacity and energy density that can be reached with device 1 shown in Fig. 4. The super capacitance exhibited: 2,230 F; 1,320 F/g<sub>cell</sub> and 44,800 F/g<sub>carbon(-)</sub> (in the

negative electrode) is another characteristic of these devices that will allow numerous practical applications.

[0019] In Fig. 5 and in the zoom in Fig. 6 the cell voltage reached is much higher and the device starts charging at 7.6 V, although it drops to 6 V subsequently to increase to 10 V afterwards. From 6-10 V the voltage increase tends to linearity. It is believed that in these cycles there is a battery mode charge/discharge corresponding to the overall stoichiometric electrochemical reaction  $(\frac{1}{8}S_8 + 2NaC_6 \stackrel{\longleftarrow}{\longleftarrow} Na_2S + 2C_6)$  corresponding to a Gibbs energy of  $\Delta G \approx -376$  kJ/mol

(corresponding to a cell voltage of 1.95 V at 298 K) and a theoretical capacity of 372 mAh/g<sub>carbon(-</sub> governed by the carbon electrode ( $NaC_6 \stackrel{\longleftarrow}{\longleftarrow} Na^+ + \bar{e} + C_6$ ). It can be observed in all the

discharges shown in Fig. 5 a hump after burst discharge that does not exceed 0.91 V. Although the expected battery mode discharging voltage is 1.95 V at 298 K. The value of x in  $Na_xC_6 \longleftrightarrow xNa^+ + x\bar{e} + C_6$  corresponding to an overall reaction  $(\frac{x}{8}S_8 + 2Na_xC_6 \longleftrightarrow xNa_2S + \frac{x}{discharge})$ 

 $2C_6$ ) and of the irreversibility percentage was previously described by (25).

[0020] Figure 7 shows charge/discharge cycles for device 2@a. In experiment a, after 20 cycles, this device shows a very similar behavior to device 1@c, after 15 cycles. While the charging current for device 1@c was 25 mA, 15mA/g, for device 2@a was 15 mA, 8mA/g. The discharge is essentially different. Device 1@c shows a hump at 0.91 V, device 2@a shows a flat voltage after burst discharge that is observed at 2.46 V and that decreases to 0.91 V during the first cycle of the experiment. It is not very clear if there is a small hump at 0.91 V as in device 1@c, but the first part of the discharge, after burst, seems to be due to the formation of the EDLCs, as will be subsequently explained.

[0021] Figure 8 shows the current explanation for the physical and chemical processes in the device during galvanostatic charge and discharge. In Fig. 8(1), at the carbon electrode and after the electron conduction and their accumulation at the surface, an EDLC(a) is formed with the separator electrolyte's Na-ions accumulating at the interface. This process leaves Na-ions holes (vacancies) on the opposite surface of the separator electrolyte (at the positive electrode interface), which correspond to a negative net charge. At the sulfur<sub>based</sub> electrode, 46 wt% of the electrode is comprised of the sodium-rich electrolyte whose Na-ions accumulate at the surface. These Na-ion vacancies within the separator electrolyte, constitute the EDLC(b) at the positive electrode's interface. At the electrode/collector interface another EDLC(c) forms from the Na-ion

vacancies on the sulfur<sub>based</sub> electrode and the positive ions at the Al collector. Figure 2 presents charge curves that seem to be in agreement with the Fig. 8(1) charging process.

[0022] In Fig. 8(2), the Na-ions of the electrolyte at the carbon electrode initiate diffusion into the electrode. The inbound ions within the carbon electrode will be reduced by the electrons and  $Na_xC_6$  will be formed. The carbon electrode, which is composed of amorphous carbon, determines the battery mode's maximum capacity has referred previously. The charge of the battery mode is not clear in the performed experiments since the EDLCs are always present during charge. However, the discharge data, indicates that battery charge took place within the Li-devices (26).

[0023] In Fig. 8(3), it is presented an explanation for the device's discharge process. The electrolyte's Na-ions in the positive electrode EDLC(c) will receive the electrons transported via external circuit from the negative electrode which will reduce and react with sulfur, leaving vacancies at the inner surface of the positive electrode. A EDLC(b) will be formed at the sulfur based electrode's interface with the Na-ions in the separator electrolyte and the vacancies of the electrode's electrolyte. On the negative electrode's side, oxidized carbon and/or the Na-ions that eventually remained after battery discharge will form another EDLC(a) with the Na-ions vacancies in the electrolyte (corresponding to a negative net charge). In Fig. 6, it is observed that once the EDLCs have burst discharged at  $V_{OC}$ , the battery mode will begin discharging. In Fig. 9 and 10, after burst discharge, the battery mode starts its discharge at  $\approx$ 3 V and the device reaches a steady rate of 1.5 V after 12 or 21 hours of discharge. This second and long discharge mode is defined as the battery mode, it can include battery and additional EDLCs formations, as shown in Fig. 8(3).

[0024] In Fig. 10 conversely to what it could observe with Li-devices (26), there is no visible  $\Delta V$  loss at discharge corresponding to the internal resistance. The resistance in Na-devices is usually an order of magnitude lower than in Li-devices (26).

[0025] The polarization inversion in Fig. 8(4) occurring during galvanostatic discharge at negative current is observed in a charge/discharge experiment with device 1, presented in Fig. 11.

[0026] It is highlighted the performance of the EDLC mode in device 1@a. The supercapacitor mode of these devices can store more energy than any other known capacitor. For simplicity, it is consider the device to be in battery mode after the discharge burst although the EDLCs that charge in this mode contribute considerably to its discharge time, as previously discussed.

[0027] The present disclosure relates to devices that are safe, environmentally friendly and inexpensive. The present devices are both supercapacitors and batteries. The switching between the two modes on charge and discharge is autonomous. The EDLCs important discharge takes place in less than or in 1 second. It is likely that other EDLCs are formed at discharge which proportionate

a delay of the battery mode discharge. Moreover, it was observed that it is possible to charge the devices during galvanostatic discharge. The present devices, working in battery mode, are uniquely charged/discharged from the Na present in the electrolyte; in effect, the sulfur at the positive electrode will only react with the Na-ions of the electrode's electrolyte protecting the electrodes interface and avoiding polysulfide shuttle. The Na-ions never cross this latter surface even during battery mode discharge. No substantial variation of the device's temperature was observed while running experiments (a maximum of 0.5 °C at 9V). The devices performed more than 30 cycles and sustained a shelf life of five months. It will be possible to tailor these devices by changing relative compositions, and by optimizing each component of the device. The capacitor or battery mode properties will depend on the previous parameters and therefore will be adapted in view of an application.

[0028] The present device is a combined EDLCs and carbon-sulfur (C-S) battery cell with a superionic sodium-rich doped Na<sub>3</sub>ClO based glassy electrolyte. In order to properly characterize the cell, two identical devices for study under different testing conditions were fabricated. These devices' in their battery modes, are charged from the high sodium content in the solid electrolyte, the only material initially containing sodium ions. Each storage device is sequentially charged as an EDLC and battery and then finally as an EDLC. This order is reverted during discharge. It is an autonomous switching dual functioning device, which can present a device voltage of 9-10 V (once the supercapacitor is fully charged). In supercapacitor mode, one device has been measured as an EDLC with a power density of 3,636 W/cm<sup>3</sup> ( $2.68 \times 10^6$  W/kg<sub>cell</sub>) for an energy density of 1.010 Wh/cm<sup>3</sup> (746 Wh/kg<sub>cell</sub>), corresponding to a discharge time of approximately 1 s (burst C-rate = 3,168C for a discharge current of 2,788 A).

[0029] In an embodiment, the present disclosure relates to a supercapacitor and battery solid carbon-sulfur Na-ion based device with autonomous dual functionality and charged from the Narich glassy electrolyte.

[0030] The present disclosure relates to a layered electrochemical solid device comprising a positive electrode current collector, a positive electrode, a glass electrolyte, a negative electrode and a negative electrode current collector wherein

the positive electrode current collector comprises aluminium;

the positive electrode comprises sulfur, a glass electrolyte of formula  $Na_{3-2x}M_xHalO$  or  $Na_{3-2x}M_xHalO$  and carbon;

the glass electrolyte composition comprising a compound of formula  $Na_{3-2x}M_xHalO$  or  $Na_{3-2x}M_xHalO$  wherein:

M is selected from the group consisting of boron, aluminium, magnesium, calcium, strontium, barium;

Hal is selected from the group consisting of fluoride, chloride, bromide, iodide or mixtures thereof;

X is the number of moles of M and  $0 < x \le 0.01$ ;

the negative electrode comprises a carbonaceous material;

the negative electrode current collector comprises copper.

[0031] In an embodiment, said layered device electrochemical solid device comprises a positive electrode current collector, a positive electrode, a glass electrolyte, a negative electrode and a negative electrode current collector in which the collectors may additionally be electrodes being the copper the positive electrode and the aluminium the negative electrode.

[0032] In some cases, the collectors can have a predominant role. They can function as electrodes being the copper + carbon black the positive electrode and the sulfur + glass electrolyte + carbon in aluminum the negative electrode. This configuration makes the device works reversely to what was described for charge and discharge. In conclusion, when the role of the collectors is preponderant, they may overcome the role of the electrodes, reversing the functions of the electrodes and leading to a device with inverted electrodes.

[0033] In an embodiment, the positive electrode of the above-mentioned layered electrochemical device may comprise

3-80% (w/w) of sulfur, in particular 30-50% (w/w) of sulfur;

3-80 % (w/w) of the electrolyte composition described previously, in particular 30-50 % (w/w) and

less than 20% (w/w) of a carbon, in particular less than 10% (w/w) of a carbon.

[0034] In an embodiment for better results, X may be 0.002, 0.005, 0.007 or 0.01.

[0035] In an embodiment for better results, Hal may be mixture of chloride and iodide, or chloride and bromide, or fluoride and iodide.

[0036] In an embodiment Hal may be a mixture of chloride and iodide, in particular for better results Hal may be 0.5 Cl + 0.5 I.

[0037] In an embodiment for better results, said electrodes may be suitable to be charged with Na-ions from the electrolyte.

[0038] In an embodiment for better results, the carbonaceous material of the negative electrode of the layered electrochemical device may be selected from the group consisting of carbon black, graphite, graphene, carbon nanotubes, spongy carbon, carbon foam, carbon white, carbon composite, carbon paper, carbon fibres, carbon film, printed carbon, and mixtures thereof.

[0039] In an embodiment for better results, the aluminium of the positive electrode current collector of the layered electrochemical device may be selected from the following list: an aluminium foam, aluminium film, aluminium foil, aluminium composite, aluminium wires, aluminium surface, or mixtures thereof.

[0040] In an embodiment for better results, the copper of the negative electrode current collector of the layered electrochemical device may be selected from the following list: a copper foam, copper thin film, copper foil, copper composite, copper wires, copper surface, other engineered form of copper, or mixtures thereof.

[0041] In an embodiment for better results, the positive electrode may further comprise an alcohol, an organic solvent, a polymer, or mixtures thereof, preferably the alcohol may be ethanol, methanol, or mixtures thereof; more preferably the alcohol may be absolute methanol, absolute ethanol, or mixtures thereof.

[0042] In an embodiment for better results, the layered electrochemical device now disclosed may further comprise a confinement, protection or wrapping immersement, said confinement, protection or wrapping immersement may by a polymer or a resin. Preferably, said polymer may be a water-proof polymer, or a water-resistant polymer, or a flexible polymer, or a rigid polymer, or a non-flammable polymer; or said resin may be an epoxy resin.

[0043] The present disclosure also relates to a capacitor comprising the layered electrochemical solid device now disclosed and described.

[0044] Furthermore, the present disclosure also relates to a battery comprising the layered electrochemical solid device now described.

[0045] The present disclosure further relates to a dual mode battery comprising the layered electrochemical solid device.

[0046] Another aspect of the present disclosure further relates to an electrical actuator comprising the layered solid electrochemical device now described.

[0047] Another aspect of the present disclosure also relates to a sonar comprising the layered electrochemical solid device now described.

[0048] Another aspect of the present disclosure also relates to a transducer comprising the layered electrochemical solid device now described.

[0049] Throughout the description and claims the word "comprise" and variations of the word, are not intended to exclude other technical features, additives, components, or steps. Additional objectives, advantages and features of the solution will become apparent to those skilled in the art upon examination of the description or may be learned by practice of the solution.

## **Brief Description of the Drawings**

[0050] The following figures provide preferred embodiments for illustrating the description and should not be seen as limiting the scope of present disclosure.

[0051] **Fig. 1:** X-ray diffraction (XRD) patterns of the carbon black negative electrode showing amorphous carbon and graphite.

[0052] **Fig. 2:** Galvanostatic charge/discharge characterization cycles for device 1 during experiment a, which was performed after 10 galvanostatic charge/discharge cycles.

[0053] **Fig. 3:** Galvanostatic charge curve for device 1 during experiment a (the same of Fig. 1). This curve is the third charging curve shown in Fig. 1. The goal is to highlight capacity and energy density.

[0054] **Fig. 4:** Galvanostatic charge curve for device 1 during experiment a (the same of Fig. 1). This curve is the third charging curve shown in Fig. 1. The goal is to highlight the device's capacitance.

[0055] **Fig. 5:** Galvanostatic charge/discharge characterization cycles for device 1 during experiment c, which was performed after 15 galvanostatic charge/discharge cycles (including experiment a). In these experiments, for the same charging current of 25 mA, the voltage reaches 10 V. It can be observed a small hump after burst discharge that it is attributed to the battery mode discharge.

[0056] **Fig. 6:** Galvanostatic charge curve for device 1 during experiment c (the same of Fig. 4). This curve is the first charging curve shown in Fig. 4. The goal is to highlight the initial voltage, the initial voltage drop to 6 V and the small hump after burst discharge that it is attributed to the battery mode discharge even if it cannot clearly identify the battery mode charge.

[0057] **Fig. 7:** Galvanostatic charge/discharge characterization cycles for device 2 during experiment a, which was performed after 20 galvanostatic charge/discharge cycles. In these experiments, performed at a charging current of 15 mA, the voltage reaches approximately 10 V.

It cannot be observed any hump after burst discharge eventually meaning that a new EDLC was formed, not letting the battery mode discharge.

[0058] **Fig. 8:** Simplified schematic representation of the processes occurring during galvanostatic charge/discharge of the present devices.

[0059] **Fig. 9:** Galvanostatic charge/discharge characterization cycles for device 2 during experiment b, which was performed after 24 cycles (including those in Fig. 6). In these experiments, performed at a charging current of 15 mA, the voltage reaches approximately 10 V. A hump cannot be observed after burst discharge meaning that a new EDLC was formed, not letting the battery mode discharge.

[0060] **Fig. 10:** Discharge burst characterization (I  $\approx$  0 mA) for device 2 during experiment b, which was performed after 24 galvanostatic charge/discharge cycles (including those in Fig. 6). It cannot be observed a  $\Delta V$  corresponding to the capacitor's mode internal resistance. **(A)** Discharge of the first cycle in Fig. 8. **(B)** Discharge of the second cycle in Fig. 8. **(C)** Discharge of the third cycle in Fig. 8.

[0061] **Fig. 11** Initial galvanostatic charge/discharge cycles performed on device 1 (this experiment was performed before a). Evidence of polarization inversion and of charge while "discharging". [0062] **Fig. 12** Schematic representation of the equivalent circuit after open circuit's discharge correspondent to Fig. 7(3).  $R_{\Omega} = 2R_e + R_i$ .

## **Detailed description**

[0063] The materials and methods are now disclosed.

[0064] In an embodiment, the synthesis of  $Na_{3-2*0.005}Ba_{0.005}CIO$  of was performed as follows: the glassy electrolyte was prepared from the commercial precursors (Panreac > 99.9 % for analysis), NaOH (Merck > 99 %) and  $Ba(OH)_2.8H_2O$  (Merck 98.5%) as described in [23,27]. After synthesis the electrolyte was heated to 100-300 °C for one hour and then cooled down, avoiding contamination with water from the air's moisture. A slurry was then prepared by grinding the electrolyte in ethanol (Merck 99.9% absolute for analysis).

[0065] In an embodiment, the preparation of the electrodes was performed as follows: the positive electrodes were prepared by adding sulfur, S<sub>8</sub>, (Alfa Aesar Powder 99.9995% Puratronic) to the above prepared electrolyte (before mixing it with ethanol) and to carbon black (TIMCAL super C65) in a 47:46:7 weight ratio. The carbon black's XRD (Fig. 1) shows the presence of graphite and amorphous carbon, probably denoting grains with an external crystalline layer and an

amorphous inner phase [28]. This mixture was grinded in ethanol (Merck 99.9% absolute for analysis). There were no prior perceptible reactions between the sulfur, the electrolyte and the graphite as presented in the XRD but the electrolyte could have reacted partially and form an amorphous phase that could not be distinguished from the amorphous electrolyte and carbon. The slurry was deposited on an Aluminum (Al) collector foil (Alfa Aesar Foil 99.45% 0.025 mm thick) with 2.50×2.50 cm<sup>2</sup> or 2.50×3.45 cm<sup>2</sup> and let dry at approximately 50-150 °C for 30 min, in particular corresponding to 40-80 mg/cm<sup>2</sup> of positive electrode. The electrolyte's slurry was deposited on the top of the positive electrode and let dry for approximately 50-150 °C for 30 min, in particular corresponding to 100-300 mg/cm<sup>2</sup> of electrolyte. The negative electrode was prepared by mixing carbon black from TIMCAL super C65 with ethanol (Merck 99.9% absolute for analysis) in a 12:88 weight ratio. The resulting slurry was deposited on a copper (Cu) collector foil (Alfa Aesar Foil 99.8% 0.025 mm thick) and let dry for about 10-20 min at 50-150 °C, in particular corresponding to 8-14 mg/cm<sup>2</sup> of carbon. The device is then prepared by matching the two collectors resulting in a layered device with Al collector/positive electrode/electrolyte/negative electrode/Cu collector. The resulting active devices were 0.15-0.35 cm thick. The device was then hermetically sealed in a moisture and oxygen free container. Collectors' terminals were left with external access.

[0066] In an embodiment, X-ray diffraction measurements were made. Samples of the positive and negative electrodes and electrolyte were submitted to X-ray Diffraction (XRD) in a Panalytical instrument, using CuK $\alpha$  radiation ( $\lambda$  = 1.54 Å) with 0.2° 2 $\vartheta$  steps and 0.5 s dwelling time, to determine the amount of the product present in the sample.

[0067] In an embodiment, electrochemical measurements were made. Galvanostatic cycling, cyclic voltammetry (CV), and electrochemical impedance spectroscopy (EIS) were performed using a SP240 potentiostat (Bio-Logic, France). Galvanostatic cycling was performed at 0.2-1.8 mA/g and between the potential limits of –10 V to 10 V versus Na/Na<sup>+</sup> and Na<sup>+</sup>/Na. The CV was performed using scan rates that ranged from 1 mV/s to 500 mV/s. The EIS was performed at open circuit voltage, with a sinus amplitude of 10 mV, and frequencies that ranged from 100 mHz to 5 MHz. [0068] In an embodiment, open circuit voltages (at fabrication, with battery mode charged and after discharge) were additionally measured with commercial multimeters.

[0069] In an embodiment, conductivity, resistance and permittivity calculations were made. The ionic conductivity, resistance and permittivity of the crystalline and glassy electrolyte may be measured using gold block electrodes and calculated using the equivalent circuits described in [23].

[0070] In an embodiment, for the devices, the equivalent circuit in Fig. 12 should be a reasonable model for three double layer capacitors (with capacitances  $C_c$  – EDLC at the interface of carbon electrode and  $C_s$  – EDLC at the interface of the sulfur<sub>based</sub> electrode and  $C_{scol}$  - EDLC inner sulfur<sub>based</sub> electrode and aluminum collector) in parallel with their charge transfer resistance ( $R_c$   $R_s$  and  $R_{scol}$  respectively) and three additional resistances in serial ( $R_\Omega = 2R_e + R_i$ ) corresponding to the ohmic drop at the electrodes and electrolyte.

[0071] In an embodiment, the Laplace transform was chosen for the study of the equivalent circuit in Fig. 12, characterized by its transfer function. In this case the impedance, Z(s), of a dipole is the transfer function for the current input  $Z(s) = \frac{\mathcal{L}\{\Delta V(t)\}}{\mathcal{L}\{\Delta I(t)\}} = \frac{\Delta V(s)}{\Delta I(s)}$  with  $\Delta V = V(t) - V(0)$  and  $\Delta I = I(t) - I(0)$ . A galvanostatic charge corresponds to a Heaviside step function response which is 0 for t < 0 and 1 for t > 0. The Laplace transform of a Heaviside step function current is given by  $\Delta I(s) = \mathcal{L}\{\delta I(t)\} = \frac{\delta I}{s}$ . The  $Z_{eq}(s)$ , for the circuit in Fig. 12, is:

$$Z_{eq} = R_{\Omega} + \frac{R_C}{SR_CC_C + 1} + \frac{R_S}{SR_SC_S + 1} + \frac{R_{Scol}}{SR_{Scol}C_{Scol} + 1}$$
(3)

$$V(s) = Z_{eq}I(s) = \frac{\delta I}{s} (R_{\Omega} + \frac{R_C}{sR_CC_C + 1} + \frac{R_S}{sR_SC_S + 1} + \frac{R_{Scol}}{sR_{Scol}C_{Scol} + 1})$$
(4)

$$V(t) = \mathcal{L}^{-1} \left\{ \frac{\delta I}{s} \left( R_{\Omega} + \frac{R_C}{sR_C C_C + 1} + \frac{R_S}{sR_S C_S + 1} + \frac{R_{Scol}}{sR_{Scol} C_{Scol} + 1} \right) \right\} = \delta I R_{\Omega} + \delta I R_C \left( 1 - e^{-\frac{t}{R_C C_C}} \right) + \delta I R_S \left( 1 - e^{-\frac{t}{R_S C_S}} \right) + \delta I R_{Scol} \left( 1 - e^{-\frac{t}{R_S Col} C_{Scol}} \right)$$

$$(5)$$

[0072] The equivalent impedance (3) is used to analyze the Cole-Cole diagram and determine the Nyquist impedance resulting from EIS.

[0073] In this case, the resulting Cole-Cole diagrams would be two perfect semi-circles. However, for real systems, sometimes this is not the case. A constant phase element (CPE), Q, is then used, instead of the capacitance C. The resulting Cole-Cole diagram corresponds to a depressed semi-circle in its upper-part. The analogy between Q and C is obtained using the following equation which gives the capacitance value at the frequency corresponding to the apex of the Cole-Cole diagram.

$$C_{EDLC} = Q(\omega_C)^{\alpha - 1} \tag{6}$$

where  $\omega_C=1/(RC)^{-1/\alpha}$  (at the top of the semi-circle). The pseudo-capacitance of each EDLC is then computed.

[0074] In an embodiment, considering the association of capacitors without having into account their charge transfer resistance it can calculate the equivalent capacitance. Since the capacitors

are associated in serial, its equivalent capacitance is  $C_{eq} = C_C C_S C_{Scol} / (C_C C_S + C_C C_{Scol} + C_S C_{Scol})$ . If the capacitances are similar, then  $C_{eq} \approx C/3$ . The capacitance of each EDLC can be written:

$$C_{EDLC} = \frac{\varepsilon \times A}{d} \tag{7}$$

where  $\varepsilon$  is the permittivity at zero-frequency ( $\varepsilon = \varepsilon_r \varepsilon_0$  where  $\varepsilon_r$  is the zero-frequency relative permittivity and  $\varepsilon_0$  is the vacuum permittivity,  $\varepsilon_0 = 8.854 \times 10^{-12}$  F/m. A is the plates' surface area and d the spacing between the plates of the capacitor (the Li-ion radius or  $2 \times \text{Li-ion}$  radius, depending on the EDLC).

[0075] In an embodiment, capacitance, internal resistance, energy, power and C-rate calculations were made. The capacitance determined from the CV data is given by:

$$C = \frac{1}{\Delta V} \int \frac{IdV}{V} \tag{8}$$

The energy determined from the CV data is given by:

$$E = \Delta V \int \frac{IdV}{V} \tag{9}$$

where C is the capacitance in Farad (F), I is the current in (A), V is the rate in (V/s), V is the voltage in (V),  $\Delta V$  is the voltage window in (V), t is time in (s) and E is the energy in (J).

[0076] The capacitance determined from the galvanostatic charge/discharge data is given by:

$$C = Q \times 3,600/\Delta V_{charge/discharge} \tag{10}$$

where C is the capacitance in (F), Q is the capacity in (Ah), I is the current in (A), V is the voltage in (V), and t is time in (s). Calculations of the gravimetric capacitance in (F/g) and (F/cm<sup>3</sup>) were also performed.

[0077] In an embodiment, the internal resistance of the EDLCs and electrolyte were estimated from the voltage drop ( $\Delta V = IR_{drop}$ ) divided by the total variation in the applied current ( $I_{charge}$ - $I_{discharge}$ ) using the following equation:

$$R_i = \frac{IR_{drop}}{I_{charge} - I_{discharge}} \tag{11}$$

[0078] For example, if  $I_{charge}$  = 2.4 mA and  $I_{discharge}$  = -2.4 mA,  $I_{charge}$ - $I_{discharge}$  = 2×2.4 mA.

[0079] The energy of the device was calculated using the following equation:

$$E = \int V dQ \tag{12}$$

where E is the energy in (J), V is the voltage in (V) and Q is the capacity in (C). The energy can be given in (Wh) if the capacity is given in (Ah). The energy density is  $\frac{E}{Volume}$  in which the Volume is given in cm<sup>3</sup>.

[0080] The energy of a device's capacitor was additionally calculated using the following equation:

$$E = \frac{1}{2} \frac{C(\Delta V)^2}{3.600} \tag{13}$$

where E is the energy in (Wh or AVh), C is the capacitance in (F) and  $\Delta V$  is the discharge voltage range in (V). The energy density is  $\frac{E}{Volume}$  in which the Volume is given in cm<sup>3</sup>.

[0081] The power density of the device was calculated from the formula given in equation:

$$P = \frac{E}{\Delta t} \times 3,600 \tag{14}$$

where P is the power density in (W/cm<sup>3</sup>), E is the volumetric energy density in (Wh/cm<sup>3</sup>) obtained from equation (12) and  $\Delta t$  is the discharge time, in particular in seconds.

[0082] In an embodiment, Charge rate or discharge was expressed as a function of the experimental capacity and calculated from the formula given in the following equation:

 $\frac{c}{n}$  charge/discharge rate =  $C(experimental\ capacity\ in\ Ah)/n(number\ of\ hours)$  (15) [0083] For example, a device with a capacity of 100 mAh will be charged at a 0.024C rate, if the current charge value is 2.4 mA which corresponds to 41.7 h (charging hours).

[0084] The disclosure should not be seen in any way restricted to the embodiments described and a person with ordinary skill in the art will foresee many possibilities to modifications thereof.

[0085] The above described embodiments are combinable. The following claims further set out particular embodiments of the disclosure.

## **References and Notes:**

- 1. Vlad, A. *et al.* Hybrid supercapacitor-battery materials for fast electrochemical charge storage. *Sci. Rep.* **4**, 4315 (2014).
- 2. Ghidiu, M., Lukatskaya, M. R., Zhao, M.-Q., Gogotsi, Y., Barsoum, M. Conductive two-dimensional titanium carbide 'clay' with high volumetric capacitance. Nature, **516**, (2014).
- 3. Li, H. B. *et al.* Amorphous nickel hydroxide nanospheres with ultrahigh capacitance and energy density as electrochemical pseudocapacitor materials. *Nature Commun.* **4**, 1894 (2013).
- 4. Liu, R., Duay, J., Lane, T., Lee, S. B. Synthesis and characterization of RuO<sub>2</sub>/poly(3,4-ethylenedioxythiophene) composite nanotubes for supercapacitors. *Phys. Chem. Chem. Phys.* **12**, 4309 (2010).

5. Jung, H. Y., Karimi, M. B., Hahm, M. G., Ajayan, P. M., Jung, Y. J., Transparent, flexible supercapacitors from nano-engineered carbon films. *Sci. Rep.* **2**, 773 (2012).

- 6. Song, H. K., Lee, K. T., Kim, M. G., Nazar, L. F., Cho, J., Recent progress in nanostructured cathode materials for lithium secondary batteries. *Adv. Funct. Mater.* **20**, 3818 (2010).
- 7. Palomares, V., Serras, P., Villaluenga, I., Hueso, K. B., Carretero-Gonzalez, J., Rojo, T., Naion batteries, recent advances and present challenges to become low cost energy storage systems. *Energy Environ. Sci.* **5**, 5884 (2012).
- 8. Ellis, B. L., Nazar, L. F., Sodium and sodium-ion energy storage batteries. *Curr. Opin. Solid State Mater. Sci.* **16**, 168 (2012).
- 9. Heimann, R. B., Classic and Advanced Ceramics: From Fundamentals to Applications. John Wiley & Sons, Apr 16, 2010.
- 10. Song, W., Cao, X., Wu, Z., Chen, J., Huangfu, K., Wang, X., Huang, Y., Ji, X. A study into the extracted ion number for NASICON structured Na<sub>3</sub>V<sub>2</sub>(PO<sub>4</sub>)<sub>3</sub> in sodium-ion batteries *Phys. Chem. Chem. Phys.* **16**, 17681 (2014).
- 11. Koenig, A. A., Rasmussen, J. R. Development of a high specific power sodium sulfur cell.

  \*Proceedings of the 34th International Power Sources Symposium.\* p. 30. doi:10.1109/IPSS.1990.145783, 1990.
- 12. Auxer, W. The PB sodium sulfur cell for satellite battery applications. *Proceedings of the International Power Sources Symposium, 32nd, Cherry Hill, NJ (Pennington, NJ: Electrochemical Society).* A88-16601 04–44: 49–54. (1986).
- 13. NRL NaSBE Experiment 1997, http://www.nrl.navy.mil/media/news-releases/1997/nrls-sodium-sulfur-battery-experiment-flies-aboard-sts87. retrieved, 03-21-2015.
- 14. http://www.popsci.com/technology/article/2010-04/texas-town-turns-monster-battery-backup-power. Texas Town Installs a Monster Battery for Backup Power | Popular Science. (2010-07-14). retrieved on 03-21-2015.
- 15. Walawalkar, R., Apt, J., Mancini, R. (2007). Economics of electric energy storage for energy arbitrage and regulation in New York. *Energy Policy* **35**(4), 2558 (2007).
- 16. Stahlkopf, Karl (June 2006). Taking Wind Mainstream. *IEEE Spectrum*. retrieved 03-21-2015.
- 17. Hong, S. Y., Kim, Y., Park, Y., Choi, A., Choic, N.-S., Lee, K. T., Charge carriers in rechargeable batteries: Na ions vs. Li ions, *Energy Environ. Sci.* **6**, 2067 (2013).

18. Ong, S. P., Chevrier, V. L., Hautier, G., Jain, A., Moore, C., Kim, S., Ma, X. H., Ceder, G., Voltage, Stability and Diffusion Barrier Differences Between Sodium-ion and Lithium-ion Intercalation Materials. *Energy Environ. Sci.*, **4**, 3680 (2011).

- 19. Doeff, M. M., Ma, Y. P., Visco, S. J., Dejonghe, L. C., Electrochemical Insertion of Sodium into Carbon. *J. Electrochem. Soc.*, **140**, L169 (1993).
- 20. Stevens, D. A., Dahn J. R. High capacity anode materials for rechargeable sodiumion batteries. *J. Electrochem. Soc.* **147**, 1271 (2000).
- 21. Alcantara, R., Lavela, P., Ortiz, G. F., Tirado, J. L., Carbon Microspheres Obtained from Resorcinol-Formaldehyde as High-Capacity Electrodes for Sodium-Ion Batteries. *Electrochem. Solid-State Lett.*, **8**, A222 (2005).
- 22. Tarascon, J.-M., Armand, M., Issues and challenges facing rechargeable lithium batteries. *Nature* **414**, 359 (2001).
- 23. Braga, M.H., Ferreira, J.A., Stockhausen, V., Oliveira, J.A., El-Azab, A. Novel Li₃ClO based glasses with superionic properties for lithium batteries. *J. Mater. Chem. A*, **2**, 5470 (2014).
- 24. Bruce, P. G., Solid State Electrochemistry, Cambridge University Press, 1994.
- 25. Yabuuchi, N., Kubota, K., Dahbi, M., Komaba, S., Research Development on Sodium-Ion Batteries. Chem. Rev. **114**, 11636 (2014).
- 26. Braga, M.H., Ferreira, J.A., Murchison, A. J., An electrochemical solid carbon-sulfur Li-ion based device, provisional patent, (2015).
- 27. Braga, M.H., Ferreira, J.A., A solid electrolyte glass for lithium or sodium ions conduction. Provisional patent (2015), PCT/IB2015/051440.
- 28. Zhang, S. *et al.* Control of graphitization degree and defects of carbon blacks through ball-milling. *RSC Adv.* **4**, 505 (2014).

# WO 2016/157083 PCT/IB2016/051776 C L A I M S

- A layered electrochemical solid device comprising a positive electrode current collector, a positive electrode, a glass electrolyte, a negative electrode and a negative electrode current collector wherein
  - the positive electrode current collector comprises aluminium;
  - the positive electrode comprises sulfur, a glass electrolyte of formula  $Na_{3-2x}M_xHalO$  or  $Na_{3-3x}M_xHalO$  and carbon;
  - the glass electrolyte composition comprising a compound of formula  $Na_{3-2x}M_xHalO$  or  $Na_{3-3x}M_xHalO$  wherein:
  - M is selected from the group consisting of boron, aluminium, magnesium, calcium, strontium, barium;
  - Hal is selected from the group consisting of fluoride, chloride, bromide, iodide or mixtures thereof; X is the number of moles of M and  $0 < x \le 0.01$ ;
  - the negative electrode comprises a carbonaceous material;
  - the negative electrode current collector comprises copper.
- 2. The layered electrochemical device according to any of the previous claim wherein the positive electrode comprises 3-80 % (w/w) of sulfur, and 3-80 % (w/w) of the electrolyte composition described in any one of the previous claims and less than 20% (w/w) of a carbon; in particular less than 10% (w/w).
- 3. The layered electrochemical device according to any of the previous claim wherein the positive electrode comprises 30-50 % (w/w) of sulfur, and 30-50 % (w/w) of the electrolyte composition described in any one of the previous claims and less than 20% (w/w) of a carbon, in particular 10% of carbon.
- 4. The layered electrochemical device according to any of the previous claims wherein X is 0.002, 0.005, 0.007 or 0.01.
- 5. The layered electrochemical device according to any of the previous claims wherein Hal is a mixture of chloride and iodide, or chloride and bromide, or fluoride and iodide.

6. The layered electrochemical device according to any of the previous claims wherein Hal is Hal = 0.5Cl + 0.5l.

- 7. The layered electrochemical device according to any of the previous claims wherein the electrodes are suitable to be charged with Na-ions from the electrolyte.
- 8. The layered electrochemical device according to the previous claims wherein the carbonaceous material of the negative electrode is selected from the group consisting of carbon black, graphite, graphene, carbon nanotubes, spongy carbon, carbon foam, carbon white, carbon composite, carbon paper, carbon fibres, carbon film, printed carbon, and mixtures thereof.
- 9. The layered electrochemical device according to any of the previous claims wherein the aluminium of the positive electrode current collector is selected from: an aluminium foam, aluminium film, aluminium foil, aluminium composite, aluminium wires, aluminium surface, or mixtures thereof.
- 10. The layered electrochemical device according to any of the previous claims wherein the copper of the negative electrode current collector is selected from: a copper foam, copper thin film, copper foil, copper composite, copper wires, copper surface, or mixtures thereof.
- 11. The layered electrochemical device according to any of the previous claims wherein the positive electrode further comprises an alcohol, an organic solvent, a polymer, or mixtures thereof.
- 12. The layered electrochemical device according to the previous claim wherein the alcohol is ethanol, methanol, or mixtures thereof; preferably absolute methanol, absolute ethanol, or mixtures thereof.
- 13. The layered electrochemical device according to any of the previous claims wherein said device further comprises a confinement, protection or wrapping immersement.

14. The layered electrochemical device according to the previous claim wherein the confinement, protection or wrapping immersement is by a polymer or a resin.

- 15. The layered electrochemical device according to the previous claim wherein the resin is an epoxy or the polymer is a water-proof polymer, or a water-resistant polymer, or a flexible polymer, or a rigid polymer, or a non-flammable polymer.
- 16. A capacitor comprising the layered electrochemical solid device described in any one of the previous claims.
- 17. A battery comprising the layered electrochemical solid device described in any one of the previous claims.
- 18. A dual mode battery comprising the layered electrochemical solid device described in any one of the previous claims.
- 19. An electrical actuator comprising the layered solid electrochemical device described in any one of the previous claims.
- 20. A sonar comprising the layered electrochemical solid device described in any one of the previous claims.
- 21. A transducer comprising the layered electrochemical solid device described in any one of the previous claims.

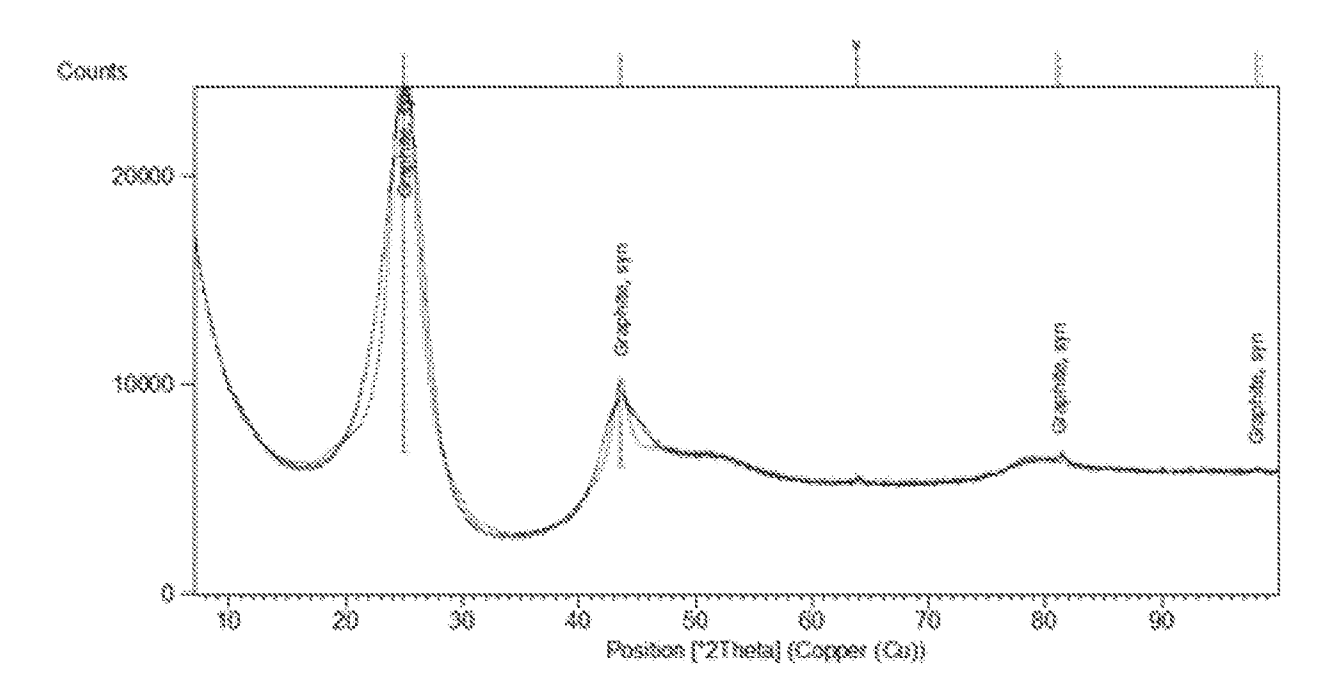


Fig. 1

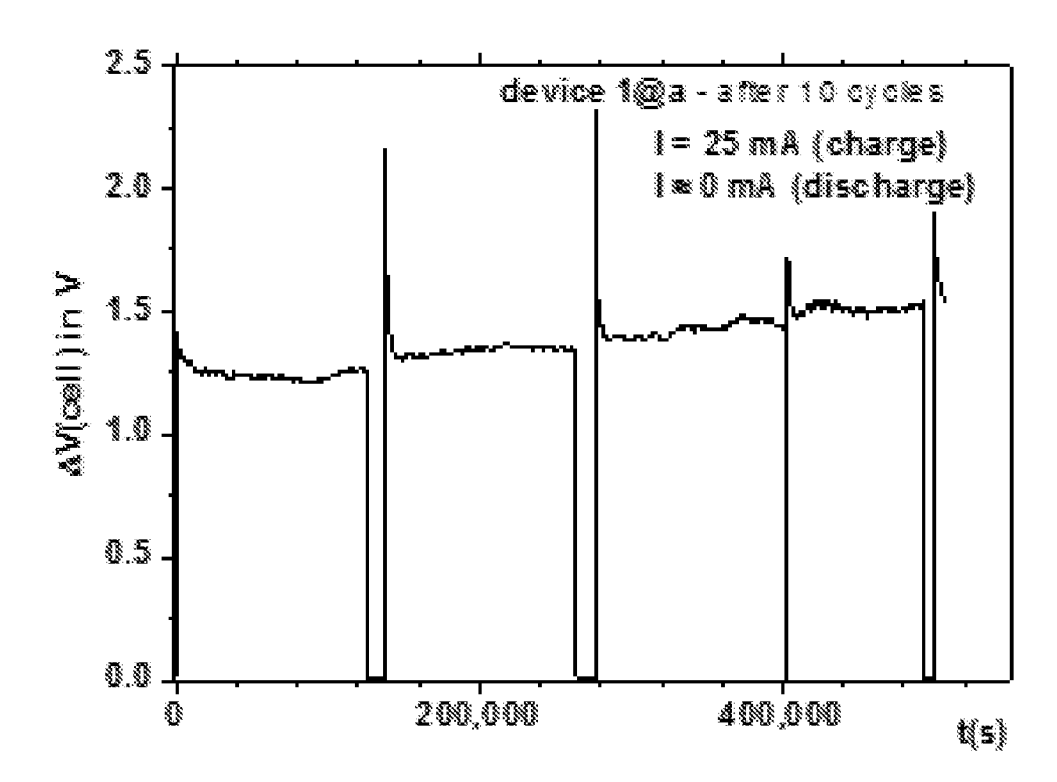


Fig. 2

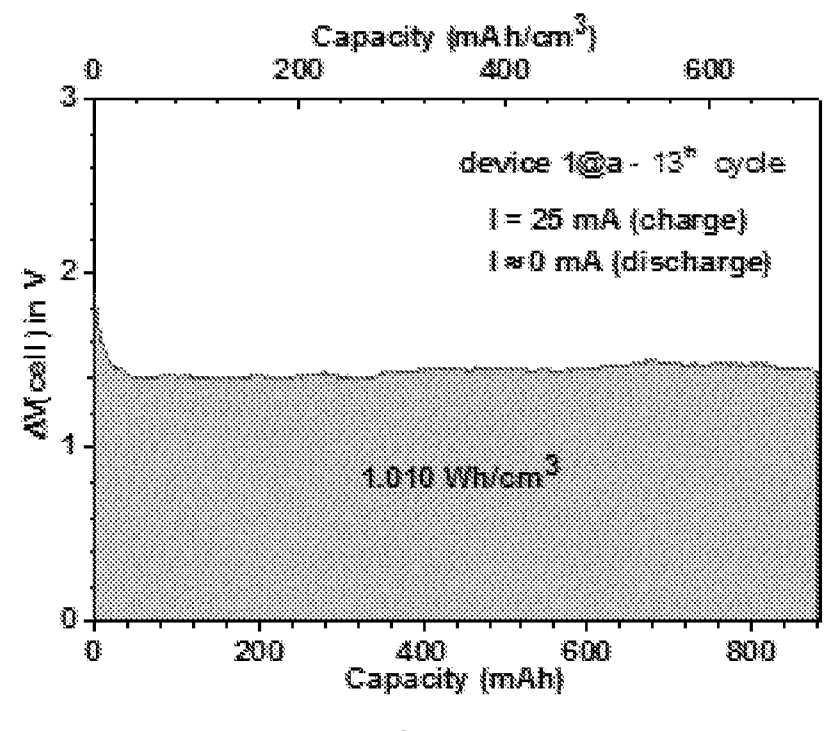


Fig. 3

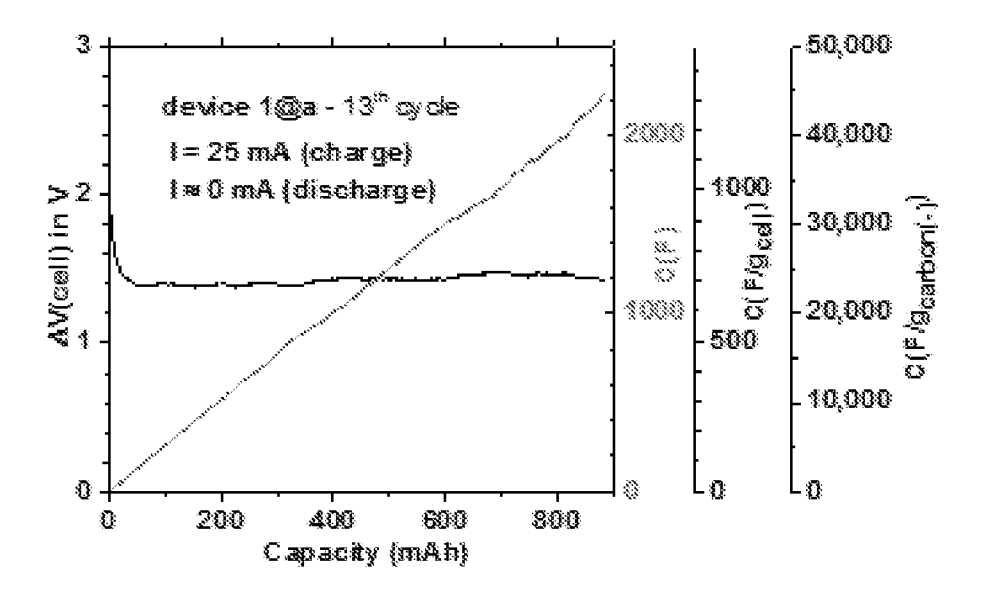
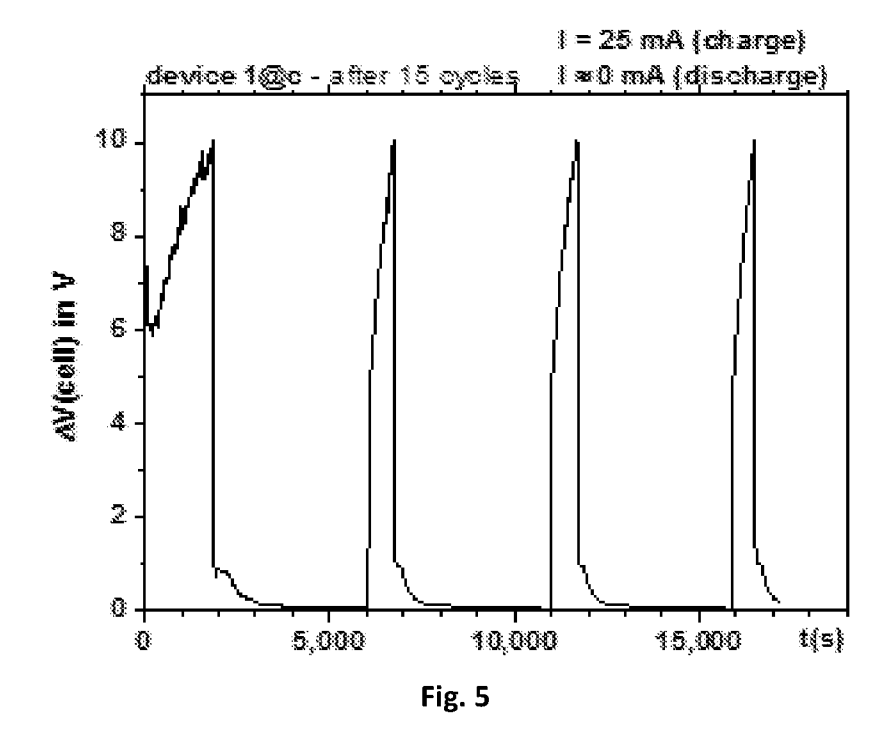
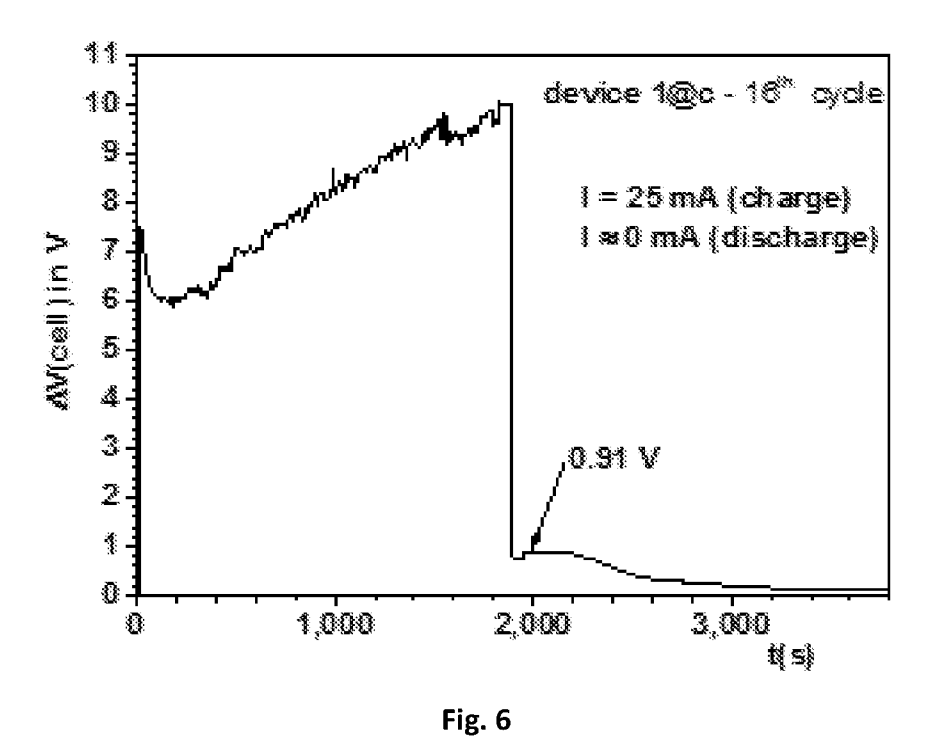


Fig. 4





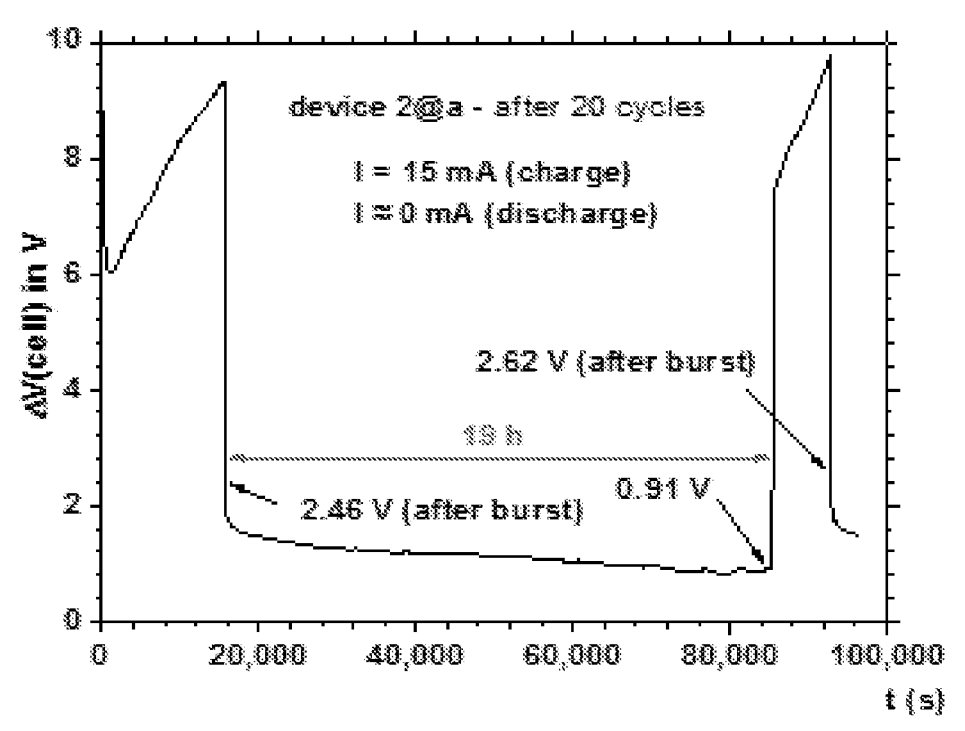
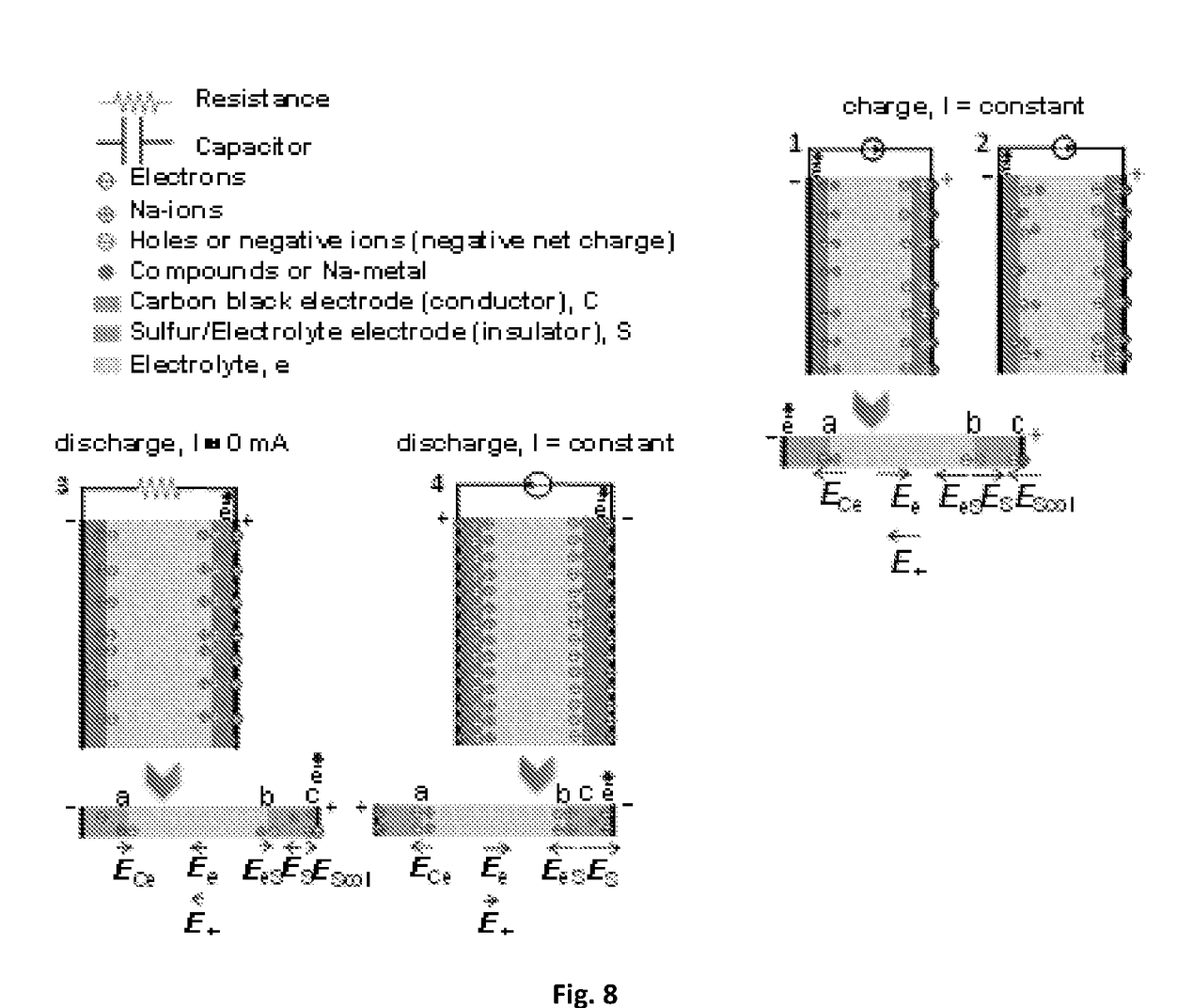


Fig. 7



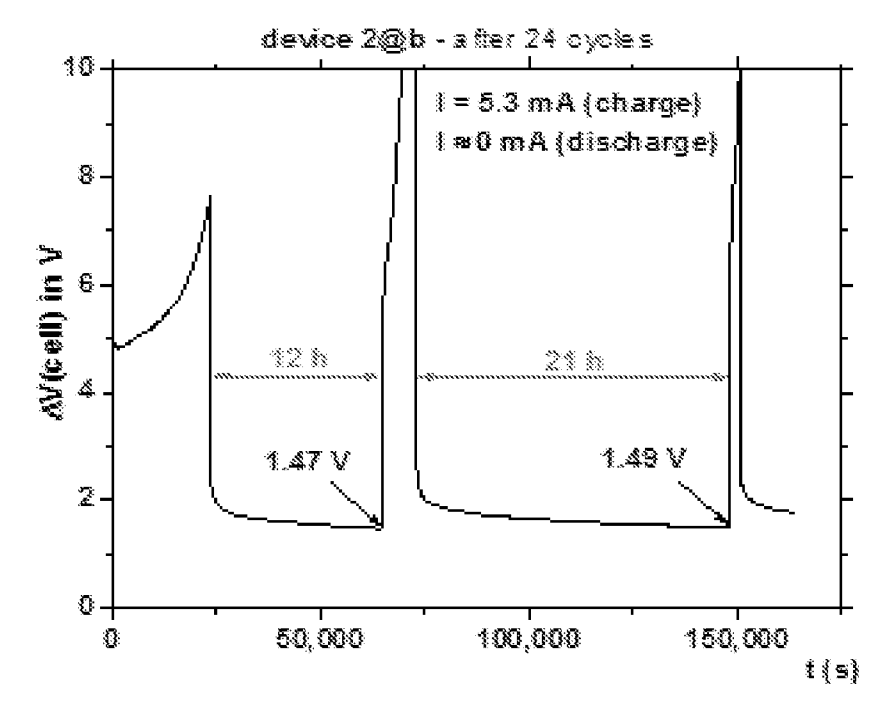


Fig. 9

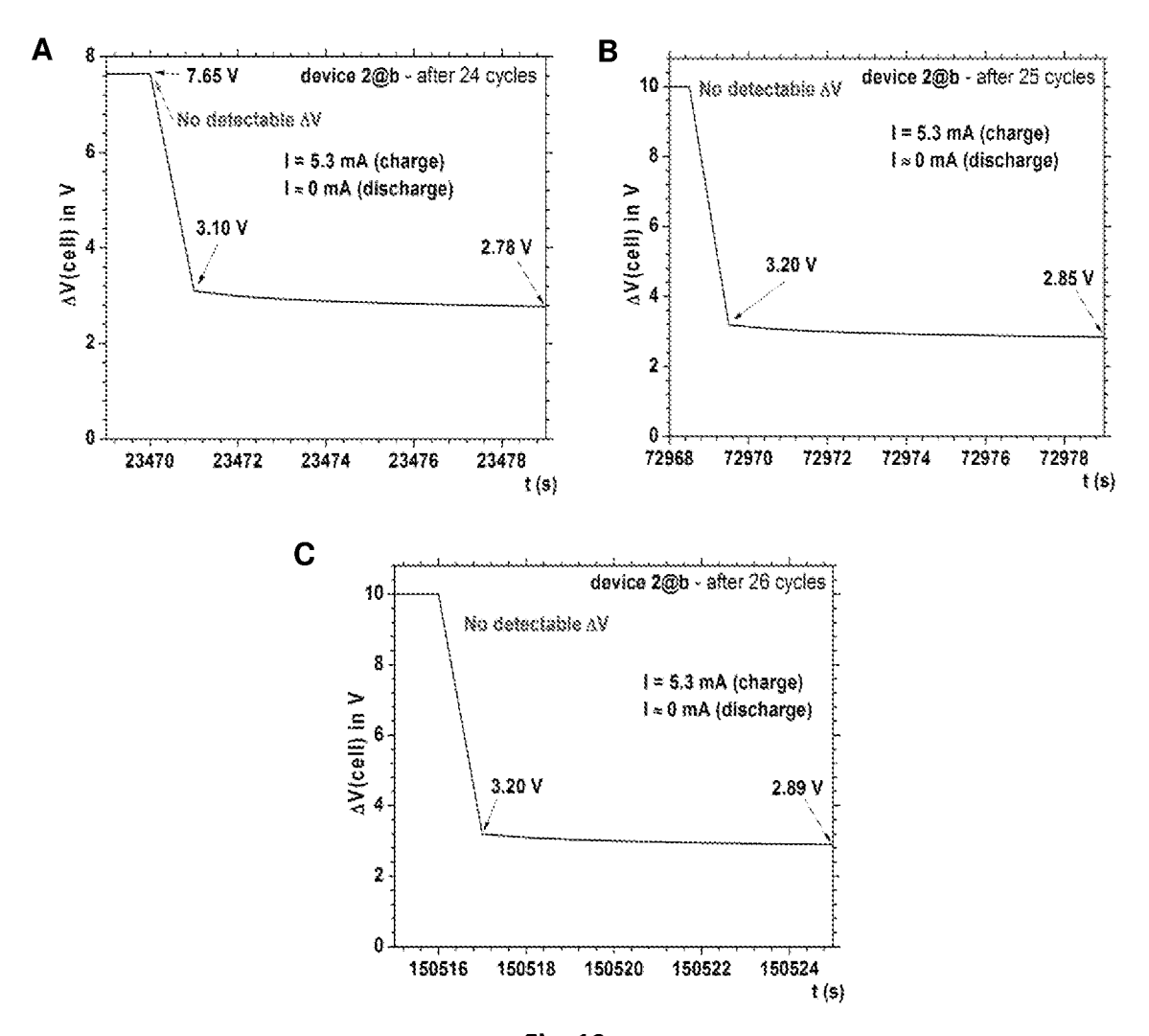


Fig. 10

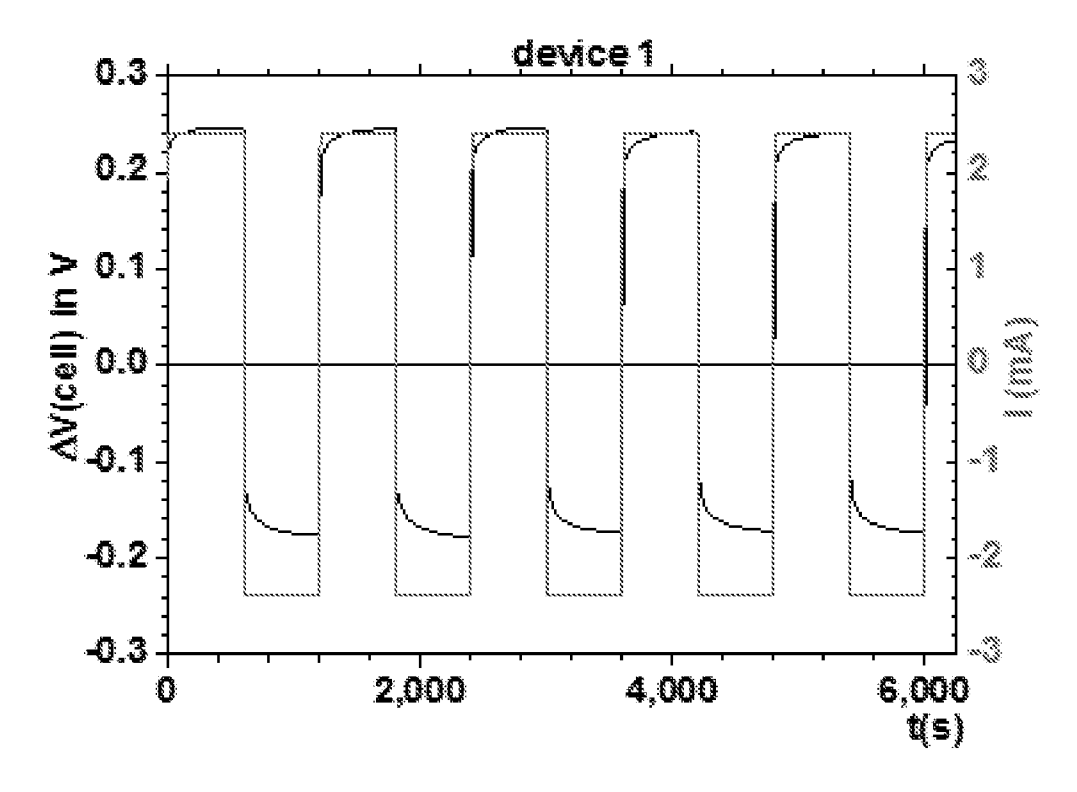
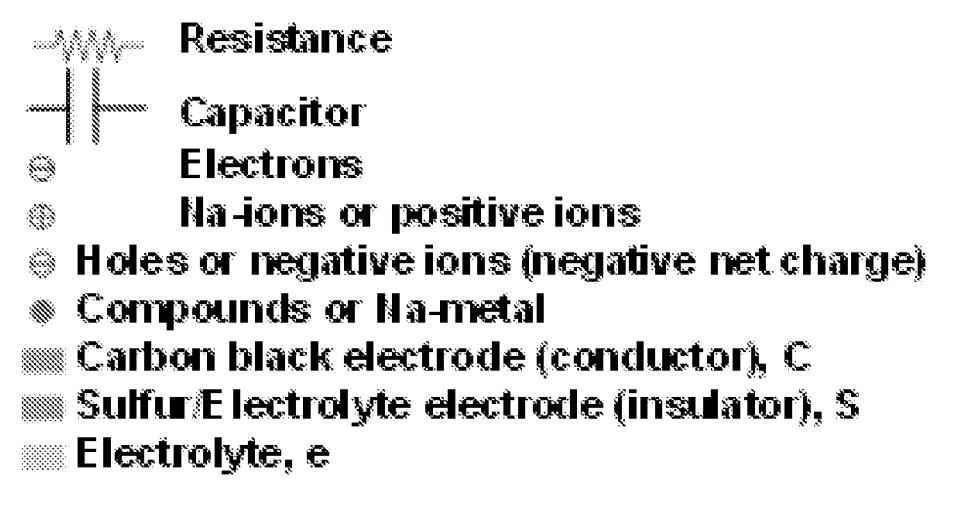


Fig. 12



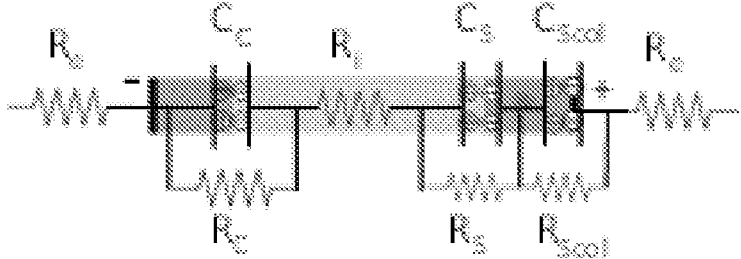


Fig. 13

#### INTERNATIONAL SEARCH REPORT

International application No PCT/IB2016/051776

A. CLASSIFICATION OF SUBJECT MATTER INV. H01M4/133 H01M4

NV. H01M4/133 H01M10/054 H01M4/136 H01M10/0562 H01M4/38 H01G9/025 H01M4/587 H01G9/15 H01M4/66

ADD. H01M2/02

H01G9/00

According to International Patent Classification (IPC) or to both national classification and IPC

#### **B. FIELDS SEARCHED**

Minimum documentation searched (classification system followed by classification symbols)

H01M H01G

Documentation searched other than minimum documentation to the extent that such documents are included in the fields searched

Electronic data base consulted during the international search (name of data base and, where practicable, search terms used)

EPO-Internal, WPI Data, CHEM ABS Data

Category*	Citation of document, with indication, where appropriate, of the relevant passages	Relevant to claim No.
Υ	WO 96/16450 A1 (POLYPLUS BATTERY CO INC [US]; CHU MAY YING [US]) 30 May 1996 (1996-05-30) abstract page 8, line 8 - line 18 page 9, line 16 - line 23 page 19, line 8 - line 16 page 22, line 19 - line 22 page 28, line 3 - line 9 claims 1-47	1-21
Υ	WO 2014/002483 A1 (IDEMITSU KOSAN CO [JP]; KOSHIKA HIROMICHI [JP]; HIGUCHI HIROYUKI [JP];) 3 January 2014 (2014-01-03) abstract -/	1-21

ı	Χ	Further documents are listed in the	continuation of Box C.
---	---	-------------------------------------	------------------------

X See patent family annex.

- \* Special categories of cited documents :
- "A" document defining the general state of the art which is not considered to be of particular relevance
- "E" earlier application or patent but published on or after the international filing date
- "L" document which may throw doubts on priority claim(s) or which is cited to establish the publication date of another citation or other special reason (as specified)
- "O" document referring to an oral disclosure, use, exhibition or other means
- "P" document published prior to the international filing date but later than the priority date claimed
- "T" later document published after the international filing date or priority date and not in conflict with the application but cited to understand the principle or theory underlying the invention
- "X" document of particular relevance; the claimed invention cannot be considered novel or cannot be considered to involve an inventive step when the document is taken alone
- "Y" document of particular relevance; the claimed invention cannot be considered to involve an inventive step when the document is combined with one or more other such documents, such combination being obvious to a person skilled in the art
- "&" document member of the same patent family

Date of mailing of the international search report

Date of the actual completion of the international search

20 June 2016

28/06/2016

Name and mailing address of the ISA/

European Patent Office, P.B. 5818 Patentlaan 2 NL - 2280 HV Rijswijk Tel. (+31-70) 340-2040, Fax: (+31-70) 340-3016 Authorized officer

Gomes Pinto F., R

# **INTERNATIONAL SEARCH REPORT**

International application No
PCT/IB2016/051776

Category*	Citation of document, with indication, where appropriate, of the relevant passages	Relevant to claim No.	
Y,P	-& EP 2 869 371 A1 (IDEMITSU KOSAN CO [JP]) 6 May 2015 (2015-05-06) abstract paragraphs [0225] - [0232], [0250] - [0254], [0278] - [0282] table 3 claims 1-4	1-21	
<b>,</b>	M. H. BRAGA ET AL: "Novel Li3ClO based glasses with superionic properties for lithium batteries", JOURNAL OF MATERIALS CHEMISTRY A, vol. 2, no. 15, 7 March 2014 (2014-03-07), page 5470, XP055194675, ISSN: 2050-7488, DOI: 10.1039/c3ta15087a abstract Introduction, 5th paragraph; page 5477, 4th paragraph; Conclusions	1-21	
,	US 2013/202971 A1 (ZHAO YUSHENG [US] ET AL) 8 August 2013 (2013-08-08) abstract paragraphs [0005], [0006], [0023] - [0025]	1-21	
A	A. PONROUCH ET AL: "Non-aqueous electrolytes for sodium-ion batteries", JOURNAL OF MATERIALS CHEMISTRY A: MATERIALS FOR ENERGY AND SUSTAINABILITY, vol. 3, no. 1, 16 October 2014 (2014-10-16), pages 22-42, XP055281928, GB ISSN: 2050-7488, DOI: 10.1039/C4TA04428B abstract 1.1 Introduction, last paragraph; 2.1 Electrolyte basics, 4th and 5th paragraphs	1-21	
A,P	YONGGANG WANG ET AL: "Structural manipulation approaches towards enhanced sodium ionic conductivity in Na-rich antiperovskites", JOURNAL OF POWER SOURCES, vol. 293, 10 June 2015 (2015-06-10), pages 735-740, XP055279752, CH ISSN: 0378-7753, DOI: 10.1016/j.jpowsour.2015.06.002 abstract 2.1 Synthesis of the NaRAP materials, figure 1	1-21	

## **INTERNATIONAL SEARCH REPORT**

Information on patent family members

International application No
PCT/IB2016/051776

Patent document cited in search report	Publication date		Patent family member(s)		Publication date
WO 9616450 A1	30-05-1996	AT AU BR CA CN DE DK EP ES JP RU US WO	0739544 0739544 2188675 H09511615 2143768	B2 A A1 A1 T2 T3 A1 T3 A C1 A	15-12-2002 17-06-1999 17-06-1996 28-10-1997 30-05-1996 26-02-1997 17-04-2003 06-01-2003 30-10-1996 01-07-2003 18-11-1997 27-12-1999 04-06-1996 02-07-1996 30-05-1996
WO 2014002483 A1	03-01-2014	CN EP JP KR TW US WO	104380508 2869371 2014011033 20150035574 201415698 2015162614 2014002483	A1 A A A	25-02-2015 06-05-2015 20-01-2014 06-04-2015 16-04-2014 11-06-2015 03-01-2014
EP 2869371 A1	06-05-2015	CN EP JP KR TW US WO		A1 A A A	25-02-2015 06-05-2015 20-01-2014 06-04-2015 16-04-2014 11-06-2015 03-01-2014
US 2013202971 A1	08-08-2013	US WO	2013202971 2014150763		08-08-2013 25-09-2014